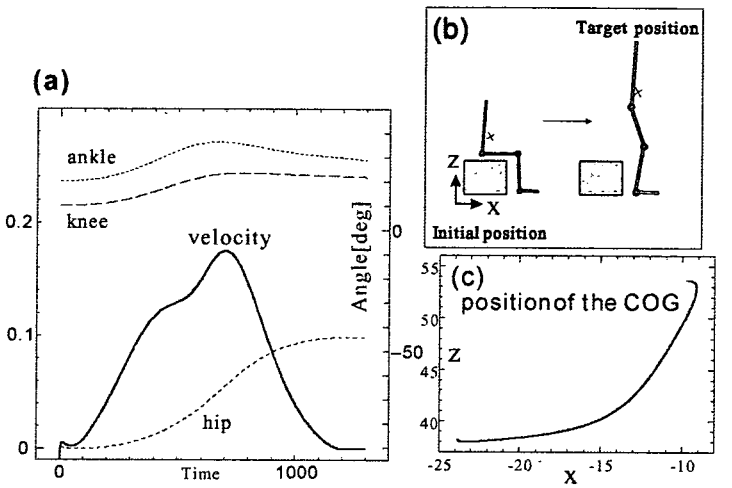

Figure 10. Standing-up movement of the four-link model. (a) Velocity transition of the COG position. (b) Initial and target states. (c) COG trajectory path from the side of the movement.

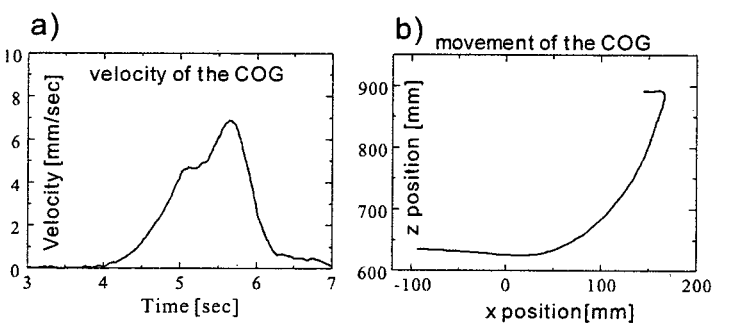

Figure 11. Optical-type motion-captured standing-up movement of a human. (a) Speed profile distribution of the COG position. (b) COG trajectory path from the side of the movement.

initial COG position in the seated state and the target position at the standing state. The reference position $\vec{x}_r$ is the midpoint between the initial and the target positions.

The speed distribution of the COG has basically one peak, and a smooth start and a convergence is seen in the speed profile curve. The COG trajectory path (from the side) is shown in Fig. 10c. Although the reference point $\vec{x}_r$ indicates the midpoint between the initial and the target points, the COG trajectory shows a slight drop due to the weight of the body and thereafter transits to the standing-up movement. These features suggest that the proposed method can handle redundant systems and can realize stable multi-link system movement. Figure 11 shows the speed profile distribution and the trajectory path of the COG movement of a human being standing-up, in which an optical motion capture system (VICON370,166 frames/s) is used. The speed profile pattern and the trajectory transition are similar.

The following experiment compares the slow-speed standing-up movement obtained by the four-link model and a human being. The simulation result of the

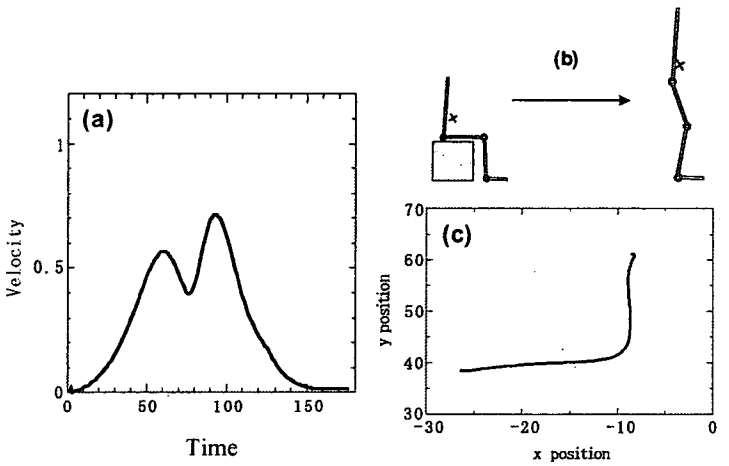

Figure 12. Slow-speed standing-up movement from a chair for the four-link model. (a) Speed transition of the COG. (b) Initial and the target states. (c) COG trajectory path from the side of the movement.

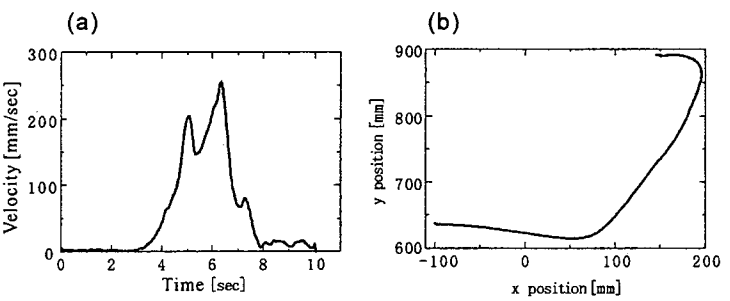

Figure 13. Motion-captured human slow-speed standing-up movement. (a) Velocity transition of the COG. (b) COG trajectory path from the side of the movement.

four-link model is shown in Fig. 12 and the human standing-up movement is shown in Fig. 13. In this experiment, the cost function parameter μ is taken as 2.0 rather than 1.0 (normal speed standing-up movement). Both movement features have two-peak speed distributions and represent a movement control strategy in which the control system first moves the COG to the support polygon and then pulls the COG up in the next phase. One- and two-peak speed profiles are found in the case of normal-speed and slow-speed standing-up movements, respectively. The reason for this is thought to be that 'the reaction' that pushes the body in the front is used for the movement [23], and in the case of normal-speed standing-up movement, when a change in the ground reaction force is observed, a rotation movement around the COG is caused by the tension applied to the floor and this rotation movement supports the standing-up movement.

Several studies examining standing-up movement have been reported in the rehabilitation field [23, 24]. The standing-up movement depends on the control

strategy used to move the COG position to the top of the foot and the COG transition process using the reaction force when the control strategy bends the body corresponds to the normal-speed standing-up movement. This difference is basically the difference between 'static standing-up' and 'dynamic standing-up', and these features can be realized by the proposed method using the cost function parameter μ. The parameter μ is a weight parameter that indicates how the acceleration of the end-effector $\vec{a}$ corresponds to the speed profile control order $\vec{f}$.

For example, if μ is large, then the acceleration $\vec{a}$ of the end-effector will be relatively small compared to the control order $\vec{f}$. This situation means that practically realized acceleration of the end-effector is small for the control order of the speed control strategy and priority is given to the system dynamics compared to the control order. This indicates that the standing-up movement is realized without giving priority to the control order for the case in which $\mu = 2.0$, compared to that in which $\mu = 1.0$.

6. MATHEMATICAL ANALYSIS OF THE TRAJECTORY PLANNING CONTROLLER

The proposed trajectory planning controller is described as:

$$m\frac{\mathrm{d}^2\vec{x}}{\mathrm{d}t} = \alpha\left\|\frac{\mathrm{d}\vec{x}}{\mathrm{d}t}\right\| \cdot (\vec{x}_\mathrm{r} - \vec{x}) + \beta(\vec{x}_\mathrm{f} - \vec{x}). \tag{12}$$

Since the second term is a simple proportional term, we do not account for this term in the present analysis, thus clarifying the role of the first term.

When the speed distribution is assumed to be defined as follows:

$$\dot{\vec{x}} = \alpha(\vec{x} - \vec{x}_\mathrm{i}) \cdot (\vec{x}_\mathrm{f} - \vec{x}), \tag{13}$$

the time differential of (13) is derived as:

$$\ddot{\vec{x}} = \alpha\dot{\vec{x}}(\vec{x}_\mathrm{f} - \vec{x}) - \alpha(\vec{x} - \vec{x}_\mathrm{i})\dot{\vec{x}} = \alpha\dot{\vec{x}}(\vec{x}_\mathrm{i} + \vec{x}_\mathrm{f} - 2\vec{x}). \tag{14}$$

By the definition of $\vec{x}_\mathrm{r} = \frac{1}{2}(\vec{x}_\mathrm{i} + \vec{x}_\mathrm{f})$, the shape of the equation structure becomes similar to that of (12), with the exception of the coefficient. In other words, (12) is used to obtain the speed distribution in the form of (13).

Here, if the speed distribution is of the form shown in (13), we can calculate the trajectory distribution by integrating (13):

$$\frac{1}{\vec{x}_\mathrm{f} - \vec{x}_\mathrm{i}}\int\left[\frac{1}{\vec{x}} + \frac{1}{\vec{x}_\mathrm{f} - \vec{x}}\right]\mathrm{d}x = \frac{1}{\vec{x}_\mathrm{f} - \vec{x}_\mathrm{i}}\left[\ln(\vec{x}) - \ln(\vec{x}_\mathrm{f} - \vec{x})\right]_{\vec{x}_\mathrm{i}}^{\vec{x}_\mathrm{f}} = K\int_{t=0}^{t}\mathrm{d}t = Kt, \tag{15}$$

where K is a constant and a very small constant Δx is introduced because (15) cannot be integrated:

$$\frac{1}{\vec{x}_f - \vec{x}_i}\left[\ln(\vec{x}) - \ln(\vec{x}_f - \vec{x})\right]_{\vec{x}_i + \Delta x}^{\vec{x}_f} = Kt. \tag{16}$$

That is, we have:

$$\frac{\vec{x} - \vec{x}_i}{\vec{x}_f - \vec{x}} = \exp K(\vec{x}_f - \vec{x}_i)t \cdot \frac{\Delta x}{\vec{x}_f - \vec{x}_i}. \tag{17}$$

By expansion about $\vec{x}$, we obtain:

$$\vec{x} = \frac{\Delta x \exp K(\vec{x}_f - \vec{x}_i)t + \vec{x}_i(\vec{x}_f - \vec{x}_i)}{\vec{x}_f - \vec{x}_s + \Delta x}, \tag{18}$$

which shows an analytical solution. Since Δx is a very small constant, the limit value is checked:

$$\begin{cases} t \mapsto 0 & \dfrac{\Delta x \cdot \vec{x}_f + \vec{x}_i(\vec{x}_f - \vec{x}_i)}{\vec{x}_f - \vec{x}_i + \Delta x} \cong \vec{x}_i \\ t \mapsto \infty & \dfrac{\Delta x \vec{x}_f}{\Delta x} \cong \vec{x}_f, \end{cases} \tag{19}$$

which means that $\vec{x}$ is in $\vec{x}_i$ at $t = 0$ and reaches $\vec{x}_f$ in time $t \mapsto \infty$. In addition, when the control term is of the shape of (12), by adding the term β, the stable equilibrium point of the system is only the point of $\vec{x}_f$ and this system causes a reaching movement to the final position $\vec{x}_f$.

We compared the proposed controller with the principle of minimum torque change (MTC) proposed by Uno *et al.* [16] from the viewpoint of ideal trajectory planning controller. The Lagrangian of 1D reaching movement under the condition of the MTC principle with friction is described as:

$$L = \frac{1}{2}\dot{f}^2 - \lambda(m\ddot{x} + k\dot{x} - f), \tag{20}$$

where f is force, $\ddot{x}$ is acceleration, $\dot{x}$ is speed, k is friction and λ is the Lagrange multiplier. By applying the principle of variation, we obtain the following set of equations:

$$\begin{cases} m\ddot{x} = -k\dot{x} + f \\ \ddot{f} = \lambda \\ \dot{\lambda} = -\dfrac{k}{m}\lambda. \end{cases} \tag{21}$$

Since $\lambda = A\exp^{-\frac{k}{m}t}$, f is given in general form as:

$$f = C + Bt + A\exp^{-\frac{k}{m}t}, \tag{22}$$

where A, B and C are constants. Here, the effect of $A\exp^{-\frac{k}{m}t}$ is thought to correspond to the friction effect and the basic structure of the MTC control can

be rewritten as follows:

$$m\ddot{x} = C + Bt. \tag{23}$$

Figure 14 shows an example of MTC control under the condtion of $C = 5$, $B = -1$ and $t_f = 10$. From (23), the velocity profile is $\dot{x} = (1/2)t(10 - t)$ and the realized position distribution is close to a sigmoidal function; however, the velocity profile was not bell-shaped. Since the general case of multi-link MTC control is affected by both internal and external dynamics or disturbances, the realized speed profile is bell-shaped. On the other hand, the proposed method has a position-dependent speed profile (13) and the dependencies of the velocity and position profile on time of the MTC are thought to be the primary difference.

Concerning the stability of the controller, letting the dispersion of the external disturbances of the system be σ, we have:

$$\sigma < \pi \cdot \gamma, \tag{24}$$

where γ is the constant of (2). This is a condition of the stability against external force disturbances $\vec{f} \longmapsto \vec{f} + \vec{e}$. The stability analysis was performed using a red noise analysis and the second fluctuation-dissipation theorem. Here, we defined the noise dispersion of $\vec{e}$ as σ (detailed proofs are not shown). In the proposed method, the parameter α determines the reaching movement speed, as described in Section 4, and β acts only to supply a small initial velocity and to hold the particle at the final position, and μ is related to the dynamics of the reaching movement, as described in Section 5. In addition, the external disturbances are represented by the γ term.

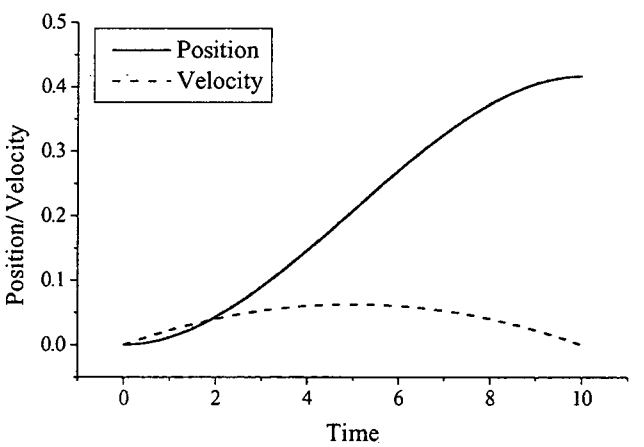

Figure 14. One-dimensional reaching movement control of minimum torque change under the condition of $t_f = 10$. The graph shows the position and velocity distribution when $f(t) = 5 - t$.

7. CONCLUSIONS

In the present paper, we propose a new control method of a multi-link arm system that was inspired by experimental results of reaching movement control in a macaque or human. In many cases, the planning and the force deciding process of previously proposed multi-link movement control methods use different algorithms and the entire multi-link dynamics cannot be managed. The proposed method unifies the trajectory planning and realization processes by exchanging the acceleration feedback information of the end-effector between these processes and the proposed method can manage external disturbances by converting the accumulation error of the trajectory realization process to the trajectory planning controller. Using this mechanism, we can determine each of the joint torques while performing the trajectory planning process and considering the dynamics of the system. The proposed method is an easy way of treating the redundant problems of multi-link system control and shows that some of the movement features of the reaching movement control are the same as those of biological systems, such as human standing-up movement.

REFERENCES

1. H. Kawamoto, S. Lee, S. Kanbe and Y. Sankai, Power assist method for hal-3 using emg-based feedback controller, in: *Proc. IEEE Int. SMC Conf.*, Washington, DC, pp. 1648–1653 (2003).
2. A. Katsnelson, Current approachs to the study of movement control, *PLoS Biol.* **1**, e50 (2003).
3. R. Volpe and P. Khosla, Computational considerations in the implementation of force control strategies, *J. Intell. Robotic Syst.* **9**, 121–148 (1994).
4. M. M. Williamson, Neural control of rhythmic arm movements, *Neural Networks* **11**, 1379–1394 (1998).
5. A. H. Fagg, N. Sitkoff, A. G. Barto and J. C. Houk, Cerebellar learning for control of a two-link arm in muscle space, in: *Proc. IEEE Conf. on Robotics and Automation*, Alburquerque, NM, pp. 2638–2644 (1997).
6. A. Hauck, M. Sorg, Schenk and G. Frber, What can be learned from human reach-to-grasp movements for the design of robotic hand-eye systems? in: *Proc. IEEE Int. Conf. on Robotics and Automation*, Detroit, MI, pp. 2521–2526 (1999).
7. T. Kashima and Y. Isurugi, Trajectory formation based on physiological characteristics of skeletal muscles, *Biol. Cybernet.* **78**, 413–422 (1998).
8. A. P. Georgopoulos, J. J. Lalaska and J. T. Massey, Spatial trajectories and reaction times of aimed movements: effects of practive, uncertainty, and change in target location, *J. Neurophysiol.* **46**, 725–743 (1981).
9. P. Morasso, Spatial control of arm movements, *Exp. Brain Res.* **42**, 2732–2743 (1981).
10. N. A. Bernstein, *The Coordination and Regulation of Movements*. Pergamon Press, Oxford (1976).
11. D. Bullock and S. Grossberg, VITE and FLETE: neural modules for trajectory formation and tension control, in: *Volitional Action*, W. Hershberger (Ed.), pp. 253–297. Elsevier, Amsterdam (1989).
12. A. Berardelli, M. Hallet, J. C. Rothwell, R. Agostino, M. Manfredi, M. Thompson, P. D. Thompson and C. D. Marsden, Single-joint rapid arm movements in normal subjects and in patients with motor disorders, *Brain* **119**, 661–674 (1996).

13. M. D. M. T. D. Sanger, Equilibrium point control of a monkey arm simulator by a fast learning tree structured artificial neural network, *Biol. Cybernet.* **68**, 499–508 (1993).
14. T. Flash, The control of hand equilibrium trajectories in multi-joint arm movements, *Biol. Cybernet.* **57**, 257–274 (1987).
15. M. Kawato, Y. Maeda, Y. Uno and R. Suzuki, Trajectory formation of arm movement by cascade neural network model based on minimum torque change criterion, *Biol. Cybernet.* **62**, 275–288 (1999).
16. Y. Uno, M. Kawato and R. Suzuki, Formation and control of optimal trajectory in human multijoint arm movement: minimum-torque change model, *Biol. Cybernet.* **61**, 89–101 (1989).
17. W. Abend, E. Bizzi and P. Morasso, Human arm trajectory formation, *Brain* **105**, 331–348 (1982).
18. A. G. Feldman, Superposition of motor programs. I. Rhythmic foream movements in man, *J. Neurosci.* **5**, 81–90 (1980).
19. H. Hogan, Impedance control; an approach to manupulation, part I to III, *ASME J. DSMC* **107**, 1–24 (1985).
20. S. Ma, Local torque optimization of redundant manupularots in torque-based formulation, in: *Proc. IEEE Int. Conf. on Industrial Electronics Control and Instrumentation*, Bologna, Vol. 2, pp. 696–701 (1994).
21. T. Flash and N. Hogan, The coordination of arm muvements: an experimentally confirmed mathematical model, *J. Neurosci.* **5**, 1688–1703 (1985).
22. W. T. Dempster, Space requirements of the seated operator, *WADC Technical Report*. Wright Patterson Air Force Base, OH.
23. J. Wheeler, C. Woodward, L. Ucovich, J. Perry and J. M. Walker, Rising from a chair: influence of age and chair design, *Phys. Ther.* **65**, 22–26 (1985).
24. R. G. Burdett, R. Habasevich, J. Pisciotta and S. R. Simon, Biomechanical comparison of rising from two types of chairs, *Phys. Ther.* **65**, 1177–1183 (1985).

ABOUT THE AUTHORS

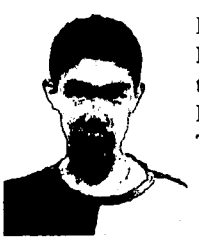

Hideki Toda belongs to the Doctoral Program of Systems and Information Engineering, Sankai Laboratory, University of Tsukuba, Tsukuba, Japan and the Multimodal Integration Research Group, Institute for Human Science and Biomedical Engineering, National Institute of Advanced Industrial Science and Technology.

Tatsu Kobayakawa belongs to the Multimodal Integration Research Group, Institute for Human Science and Biomedical Engineering, National Institute of Advanced Industrial Science and Technology.

Yoshiyuki Sankai received the PhD degree in Engineering from the University of Tsukuba, Japan, in 1987. He was named a JSPS Fellow, Research Associate and Associate Professor in the University of Tsukuba. He is a Visiting Professor at Baylor College of Medicine, USA, and an Ordinary Professor in the Institute of Systems and Engineering Mechanics, University of Tsukuba, Japan. His research interests include assistive exoskeletal robots, the next generation of artificial hearts and humanoids as related fields of cybernetics. He received the JSAO-Grant of the Japanese Society for Artificial Organs, and awards from the American Society for Artificial Organs, International Society for Artificial Organs and International Society for Rotary Blood Pump with his students. He is a Chair of the Japan Society of Embolus Detection and Treatment, Vice Chair of the International Journal of the Robotics Society of Japan, member of the Awards Committee of the Japan Society of Mechanical Engineers, and member of the Assessment Committee of the New Energy and Industrial Technology Development Organization, Japan.

Advanced Robotics, Vol. 21, No. 12, pp. 1441–1469 (2007)

Also available online - www.brill.nl/ar

Full paper

Intention-based walking support for paraplegia patients with Robot Suit HAL

KENTA SUZUKI [1], GOUJI MITO [1], HIROAKI KAWAMOTO [2], YASUHISA HASEGAWA [1] and YOSHIYUKI SANKAI [1,*]

[1] *Graduate School of Systems and Information Engineering, University of Tsukuba, 1-1-1 Tennodai, Tsukuba, Ibaraki 305-8573, Japan*

[2] *Japan Association for the Advancement of Medical Equipment, NKD Building, 3-42-6 Hongo, Bunkyo-ku, Tokyo 113-0033, Japan*

Received 9 January 2007; accepted 1 April 2007

Abstract—This paper proposes an algorithm to estimate human intentions related to walking in order to comfortably and safely support a paraplegia patient's walk. Robot Suit HAL (Hybrid Assistive Limb) has been developed for enhancement of a healthy person's activities and for support of a physically challenged person's daily life. The assisting method based on bioelectrical signals such as myoelectricity successfully supports a healthy person's walking. These bioelectrical signals, however, cannot be measured properly from a paraplegia patient. Therefore another interface that can estimate a patient's intentions without any manual controller is desired for robot control since a manual controller deprives a patient of his/her hand freedom. Estimation of a patient's intentions contributes to providing not only comfortable support but also safe support, because any inconformity between the robot suit motion and the patient motion results in his/her stumbling or falling. The proposed algorithm estimates a patient's intentions from a floor reaction force (FRF) reflecting a patient's weight shift during walking and standing. The effectiveness of this algorithm is investigated through experiments on a paraplegia patient who has a sensory paralysis on both legs, especially his left leg. We show that HAL supports the patient's walk properly, estimating his intentions based on the FRF, while he keeps his own balance by himself.

Keywords: Robot suit; paraplegia; walking support; intention estimation; floor reaction force.

1. INTRODUCTION

People may have muscle rigidity, relaxation, involuntary muscle contractions and sensory paralysis due to cerebral paralysis, stroke, spinal cord injury, muscular dystrophy and post-polio syndrome. Even if people do not suffer from these physical problems, aging brings various complications on their motility. Most

*To whom correspondence should be addressed. E-mail: cybernoid@golem.kz.tsukuba.ac.jp

people who have problems on the lower limbs due to these symptoms or aging are unable to walk and, at worst, are bedridden all day long. Moreover, this situation depresses a patient's feelings, e.g., bedridden patients lose their will to life. Caregivers including the patient's family also have problems looking after them once a person has motility troubles. To relieve these problems and to support the patient's independent life, it is important to provide them with a safe and convenient transportation device.

A wheelchair is now used in most cases as a transportation device for patients with gait disorder. It is convenient for the patients because they can move easily as long as enough muscular power remains in their upper body. Even if a patient has weakness of the arms, a motorized wheelchair could be used. However, wheelchairs have some problems relating to the user's environment and the user's posture. In particular, wheelchair users are apt to keep a sitting posture for a long time and have less opportunity to exercise their own lower bodies. That may cause a decrease in not only muscular power of the lower body with paralysis, but also residual physical functions. This problem could be solved if a patient with paraplegia could walk on his/her own legs as a healthy person does. Therefore, a device which helps a patient walk in their standing posture would be one of the solutions since the patient can locomote with their legs receiving physical support.

Several devices for walking support have been developed. In our study, a wearable-type robot 'Robot Suit HAL' (Hybrid Assistive Limb) has been developed in order to physically support a wearer's daily activities and heavy work. HAL-1, utilizing DC motors and ball screws as shown in Fig. 1a, was developed as the first prototype of HAL [1] and it enhanced the wearer's walking ability by amplifying the wearer's own joint torque. After developing some prototypes, HAL-3 (Fig. 1b) was developed toward a more suitable system to be used in actual daily life [2, 3]. These robot suits have a power unit on each hip and knee joint, and they support functional motions of the lower limbs with multiple joints simultaneously. After that, HAL-5 (Fig. 1c), demonstrated at the 2005 World Exposition in Aichi, was developed for whole-body support. It assists human motions involving the wearer's upper-body activities such as carrying heavy loads. Meanwhile, 'RoboKnee' [4] and 'Wearable Walking Helper' [5] have been developed to support knee motion by using linear actuators. However, it is difficult for these two devices to support a patient with paraplegia since these devices cannot support multiple joints in the lower limbs simultaneously. As an exoskeleton to assist soldiers, disaster relief workers and other emergency personnel who need to move long distances on foot, Kazerooni *et al.* [6, 7] have developed 'BLEEX' that supports a human's walking while carrying heavy loads on his/her back. This exoskeleton is not designed for welfare purposes, and it is too large and heavy (75 kg including the exoskeleton weight and maximum payload) for patients to handle as their own supporting devices in actual daily life.

To provide effective physical support according to each wearer's condition, it is necessary to strongly focus on the control algorithm as well as mechanisms of supporting devices. HAL has a cybernic control system that is a hybrid control

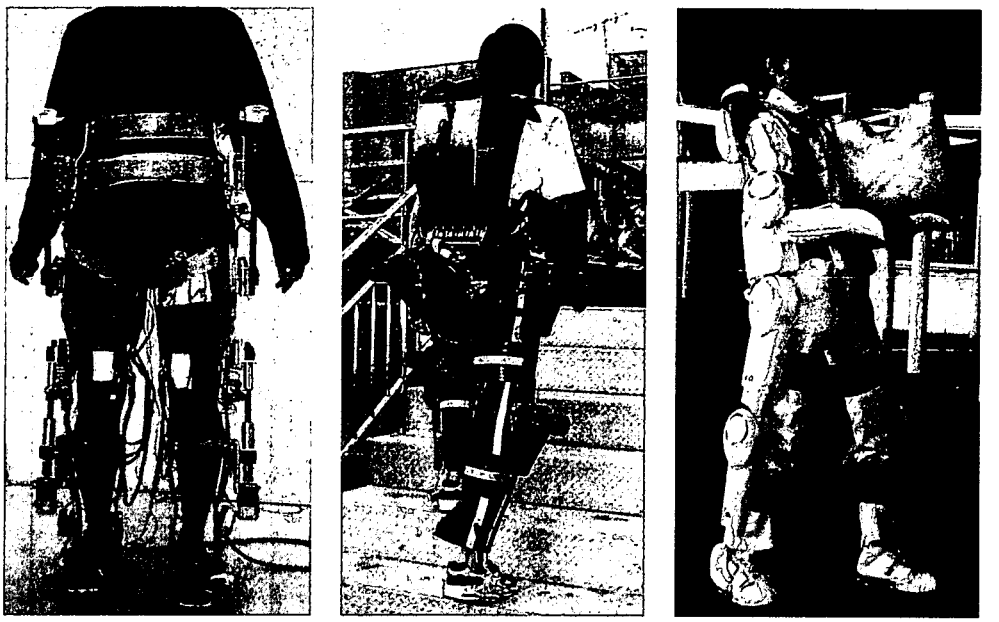

(a) HAL-1(1999). (b) HAL-3(2001). (c) HAL-5(2005).

Figure 1. Representative conventional robot suits we have developed. (a and b) HAL supports the wearer's lower-body motion. (c) HAL supports the whole-body motion. A 20-kg load is carried on a single arm.

algorithm consisting of a 'Cybernic Voluntary Control (Bio-Cybernic Control)' and 'Cybernic Autonomous Control (Cybernic Robot Control)'. The cybernic control system can provide suitable physical support to wearers in various conditions such as a healthy person, a physically challenged person, etc., by using the two algorithms as complementary controls. The features of each control algorithm are described below.

The Cybernic Voluntary Control provides physical support according to the patients's voluntary muscle activity. The power units of HAL generate power assist torque by amplifying the wearer's own joint torque estimated from his/her bioelectrical signals and the support motions are consequently controlled by signal adjustment. This control was used for power assist of a healthy person's activities [8], e.g., walking and standing up from a sitting posture, and we confirmed the Cybernic Voluntary Control successfully supported a wearer's motion. Bioelectrical signals, including myoelectricity, are useful and reliable information to estimate a human's motion intentions because the signals are measured just before corresponding visible muscle activities. Thus, the wearer receives physical support directly by an unconscious interface using the bioelectrical signals, which much more easily realize operation than manual controllers such as a joystick. HAL can physically support patients with some handicaps on their lower limbs as well as healthy people because HAL supports functional motions with multiple joints simultaneously,

covering the whole of the lower limbs. However, as a whole, a patient with a gait disorder is not able to receive walking support by the Cybernic Voluntary Control because the signals that induce a broken walking pattern are not used for the power assist, and signals from the brain are not transmitted from the injured spinal cord to the more distant parts of the body and no signal is observed on the paralyzed muscles in the severest case. In that case, the Cybernic Autonomous Control can provide an effective physical support.

The Cybernic Autonomous Control autonomously provides a desired functional motion generated according to the wearer's body constitution, conditions and purposes of motion support. While bioelectrical signals are mainly used in the Cybernic Voluntary Control, various kinds of information apart from bioelectrical signals, such as reaction force and joint angle, can be used to provide comfortable physical support. It can be applied to rehabilitation and walking support for patients as well as power assist for healthy people, and it enables HAL to be used as alternate body functions for their handicaps or weakness of muscular power. In that case, HAL needs to observe a wearer's conditions and motion intentions from any motion information instead of his/her bioelectrical signals in order to provide a suitable support with a suitable moment. HAL-3 with the Cybernic Autonomous Control successfully enhances a healthy person's walking, stair-climbing, standing up from a sitting posture and cycling, synchronizing with his/her body condition [9]. In that work, floor reaction forces (FRFs) and joint angles are used as motion information to detect a wearer's conditions. Posture control, as well as sensing and recognition for an environment including a wearer are essential technologies for an entire autonomous physical support, but they remain to be solved. In this paper, the Cybernic Autonomous Control among the cybernic control systems is applied to HAL in order to support a paraplegia patient's walking. Our conventional Cybernic Autonomous Control algorithm [9] cannot be applied to them directly due to a variety of body constitutions and handicaps.

Generally, the human intentions in his/her mind are essentially independent from the physical interactions between a body and an environment. As far as we know, no current technologies can directly measure and extract the human intentions. However, we can sometimes guess human intentions in their mind from their appearance or motion. In addition, we can estimate his/her corresponding intentions if we observe a motion or an appearance that is closely connected with his/her intentions. According to conventional work on human transient walking [10, 11], a center of gravity (COG) shift to one leg is a prior motion to a walk. That motion is indispensable to swinging a leg and can be observed earlier than a bioelectrical signal such as myoelectricity, because it is observed before a human starts swinging a leg, while a bioelectrical signal is observed when the corresponding muscles start contracting. The COG shift can be used for an early and smart trigger to start walking support, because the shift is involved in preliminary motions for a walk and a human does not have to operate any manual switch to start the walking support. On the other hand, gait stopping is similar to the time-reverse motion

of the gait initiation and the COG stops at around the center of both supporting legs. Therefore, this paper proposes an intention estimator that can estimate his/her walking intentions from the COG shift that is closely connected with his/her intention.

We define that intention-based support (including walking support) is to provide physical support for the wearer's next desired motion that can be predicted based on the current state or motion induced by his/her intention. In the case of walking, a human shifts the COG to a supporting leg side before he/she starts swinging a leg. If HAL can sense the COG shift induced by his/her intention, it can predict his/her walking start and then start walking support. Our project aims to realize comfortable walking support for paraplegia patients that reflect the patient's intentions on the start and stop of walking, cycle and stride of walking motion, walking direction, etc. We call the walking support conforming to these various intentions of walking 'intention-based walking support'. It is hoped that intention-based walking support improves the usability, safety and reliability of HAL. As the first step, this paper focuses on three kinds of intentions: the start and stop of walking and the beginning to swing a leg, and proposes a control algorithm that uses the patient's residual physical functions effectively. We need to observe not only the COG shift in the lateral plane, but also the forward COG shift and bending of the upper body in order to distinguish the gait initiation from other similar motions such as just stepping or changing a supporting leg for leg relaxation. However, HAL can understand the patient's intention if we instruct the wearer to shift the COG to either of his/her legs in order to receive physical support for swinging a leg. Therefore, the FRF can be one type of reliable information that reflects his/her intentions without any manual interface if a patient can control his/her weight balance in the lateral plane by holding a walking frame with their own hands.

The purpose of this study is that HAL helps a patient with paraplegia walk in a standing posture. Based on our conventional work, two additional functions should be developed for this purpose. First, HAL should generate suitable bipedal walking according to the patient's body constitution. Reference trajectories for each joint support should be designed in a different way because bioelectrical signals are not observed from a patient with paraplegia. The reference motions consist of swinging the wearer's leg, supporting his/her weight and shifting his/her weight from one leg to the other. Second, HAL should provide walking support according to the patient's intentions that are estimated from the wearer's COG shift. To achieve the two functions mentioned above, this paper takes the following approaches:

(i) To achieve bipedal locomotion partially based on walking patterns of a healthy person.

(ii) To estimate the wearer's intentions from his/her COG shift that is observed by the FRF.

(iii) To synchronize support motions with estimated wearer's intentions: walk start, stop and the beginning to swing a leg.

Section 2 explains the assumptions and approach of this study. Section 3 introduces the robot suit 'HAL-5 Type-C' used in this experiment. Section 4 describes the proposed algorithm for walking support and intention estimation. Section 5 shows experimental results and verifies the performance of the proposed algorithm in HAL-5 Type-C. Finally, Section 6 gives the conclusions.

2. ASSUMPTIONS AND APPROACH

In this paper, a proposed algorithm is applied to walking support for a paraplegia patient called 'participant A' in this paper. He has sensory and motor paralysis on both legs, especially the left leg because of spinal cord injury (SCI) caused by a traffic accident. He gave informed consent before participating and the experiments were conducted under the inspection of physical therapists. He can keep a standing posture and slowly walk by himself with two canes. In this case, we cannot measure proper bioelectrical signals to estimate his intention during walking because of the disorder of neural transmission. We, therefore, use the FRF instead of bioelectrical signals in this experiment. The FRF reflects his weight shift during walking and standing. It should be noted that he can control his balance holding a walking frame and that our algorithm can estimate his intentions from his FRF. That is, our algorithm synchronizes the physical support with his intentions through his controlled weight balance not by using manual controllers such as a joystick, but by using the FRF during walking and standing. The reference patterns for the patient are extracted from a healthy person's walk. The healthy person's walking motion could be suitable for the patient if he/she has the same body constitution as the healthy person. The extracted walking motion, however, should be adjusted according to the patient's body constitution and handicap conditions, e.g., the walking cycle and amplitude of each joint trajectory in swinging a leg.

3. ROBOT SUIT HAL

In the experiment, HAL-5 clinical type (HAL-5 Type-C) made for participant A was used. Figure 2 shows an overview of HAL-5 Type-C and Fig. 3 shows its system configurations. As in the case of the conventional type of HAL (HAL-3), HAL-5 Type-C consists of power units, exoskeletal frames, sensors and a controller. Power units are attached on each hip and knee joint, and actuate each joint by their torques. Springs are attached on the ankle joints so that the wearer's ankle joints could come back to a normal angle even if no external forces affect the joints. The spring action contributes to avoiding collisions between the toe of the swing leg and the floor. The exoskeletal frames are fixed to the wearer's legs with molded plastic bands and transmit the torques of the power units to his/her legs. There are angular sensors and FRF sensors to measure motion information of HAL-5 Type-C and a wearer to enable intention estimation for the wearer. Potentiometers as angular

(a) (b)

Figure 2. HAL-5 Type-C developed for walking support of a paraplegia patient. Total weight is 15 kg. (a) Back view. (b) Side view.

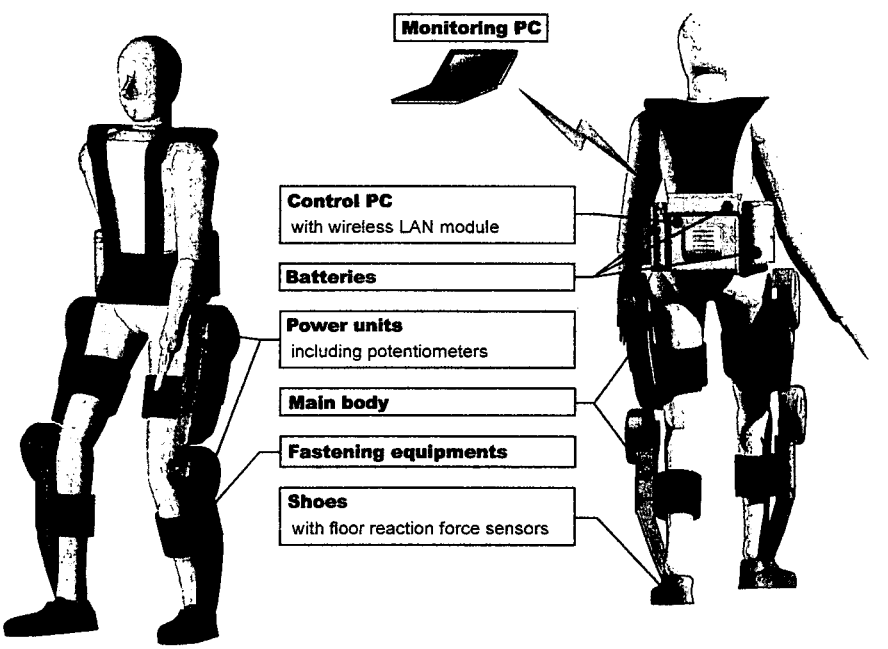

Figure 3. System configurations of HAL-5 Type-C.

sensors are attached to each joint to measure the joint angles. FRF sensors utilizing a semiconductor-type pressure sensor are implemented in shoes. Figure 4 shows the appearance of the shoes of HAL-5 Type-C with built-in FRF sensors. The weight of the wearer including HAL-5 Type-C is transferred onto the sensor unit and

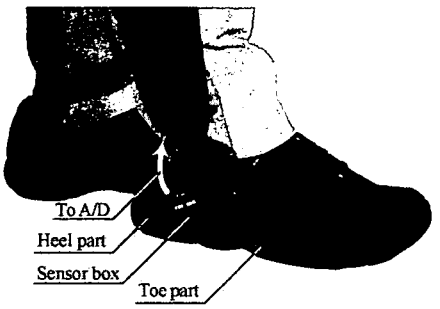

Figure 4. Built-in FRF sensors utilizing a semiconductor-type pressure sensor. These sensors can measure the distribution of load between the toe and heel parts during walking and standing because two sensors are built in the front and rear of the sole.

Figure 5. Rotation directions of each lower leg joint. Angle and angular velocity data shown in this paper shall be subject to a rule that flexion of a joint is a positive rotation and extension is a negative one, when the angles of each joint in an upright posture are set to the zero angles.

measured by the pressure sensors. These sensors can also measure the distribution of load between the toe and heel parts during walking and standing because two sensors are built in the front and rear of the sole. In addition, a computer and batteries are attached on a wearer's waist, and motor drivers and other electrical circuits for the signal processing are allocated on each power unit. Compared with HAL-3 (Fig. 1b), HAL-5 Type-C is improved for daily use since there is no large backpack on the user's back and the width of the power units in the back view becomes thin enough to pass through narrow spaces as shown in Fig. 2. Figure 5 shows angles and rotation directions of each joint described in this paper.

4. CONTROLLER DESIGN

In this section, we explain the controller for the walking support system. Walking motion in this work shall be considered to consist of three functions including swinging a leg, landing and supporting a body as shown in Fig. 6. In this paper, we call each span of three functions the swing phase, landing phase and support

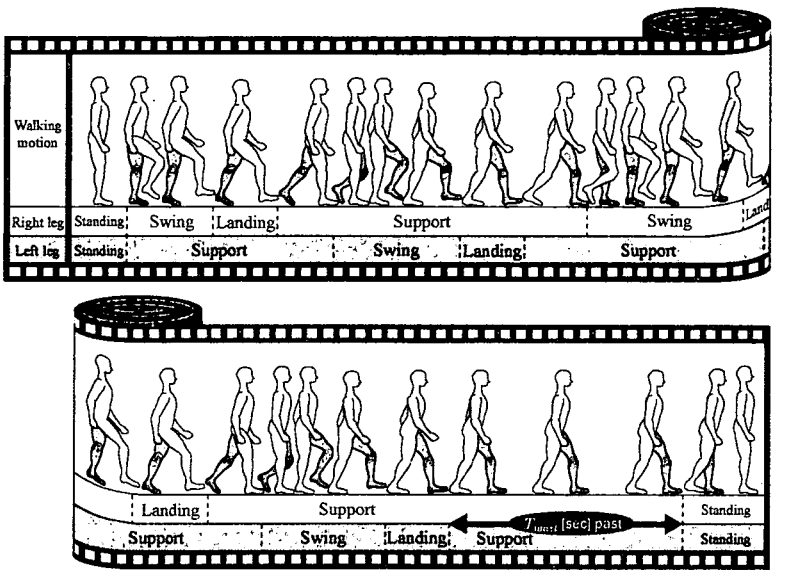

Figure 6. Three functions in walking motion: swing phase, landing phase and support phase. T_{wait} is a temporal threshold to switch the walking support to the standing posture support. If a wearer wants to stop walking in their tracks, they just have to stop weight shifting for T_{wait} seconds.

phase. In the swing phase, the patterns extracted from a healthy person's walk are applied as the reference patterns of the proportional and derivative (PD) control for the corresponding joints of a wearer. The reference patterns are used for the corresponding leg's control synchronizing with the wearer's intention estimated by our proposed algorithm. In the landing phase, we realize the leg function for a foot landing by not tracking reference patterns, but by applying constant-value control. Based on our conventional work [12], we found that the knee joint of a wearer at landing is apt to be flexed by his/her own weight and much torque beyond the torque tolerance is needed to compensate for the knee bend. Therefore, the knee joint has to be extended earlier than the reference pattern by constant-value control. In the support phase as well as the landing phase, the leg is supported by constant-value control in order to support the weight by one leg. The following sub-sections explain the details of the controller algorithm.

4.1. Reference pattern generation

As mentioned above, a swing leg in the swing phase is supported by applying reference walking patterns measured in a healthy person's walk. The reference patterns are generated in the following process:

(i) To measure angle data of the hip and knee joints in a healthy person's walk.

(ii) To divide a sequence of the measured walk pattern into patterns of each step and then average the walk patterns.

(iii) To divide the averaged pattern into three phases and extract a pattern in the swing phase.

First, we measure a healthy person's walk to acquire the angle data of hip and knee joints during walking. In this experiment, we measure the normal walk of a man in his 20s, who has a similar body constitution, including height, weight and length of legs, to participant A. Second, a sequence of the measured walk pattern is divided into patterns in each step and then the patterns averaged. At this stage, we should pay note that habits of walking and asymmetry between the right and left leg step are not strongly reflected in the extracted patterns. Figure 7a shows walking patterns in one step averaged in this experiment. Finally, the averaged walking patterns are divided into patterns in the swing, landing and support phases. The swing phase is between the moment when the foot leaves the floor and the moment when the thigh is fully flexed. The landing phase continues until the moment when the foot of the swing leg contacts the floor and the support phase continues until the moment when one step finishes. The walking patterns extracted from a healthy person's walk are shown in Fig. 7b–d. Namely, Fig. 7b shows the reference angle patterns in the swing phase used in this walking support. The PD controller to drive a leg swing needs reference angular velocity patterns as well as the angle patterns and the angular velocity patterns are generated by differentiating the angle patterns with respect to time. In addition, the time scales of the reference patterns are linearly

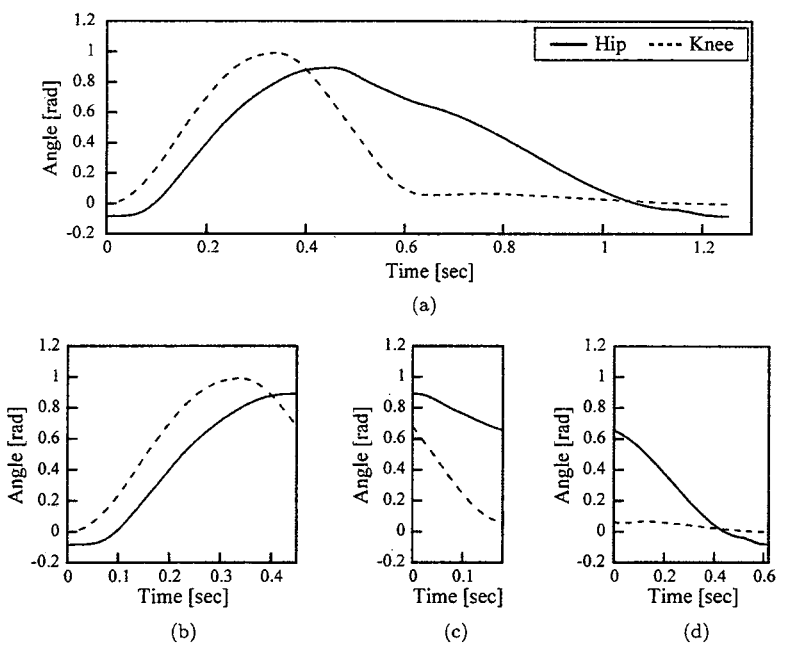

Figure 7. Reference walking patterns of joint angle. (a) Patterns in one cycle of walking. (b) Patterns in the swing phase. (c) Patterns in the landing phase. (d) Patterns in the support phase.

Table 1.
Reference values in one cycle of walking support

	Swing phase	Landing phase	Support phase
θ_{href} (rad)	Fig. 7b	0.0	0.0 (−0.7)
$\dot{\theta}_{\text{href}}$ (rad/s)	time derivative of Fig. 7b	0.0	0.0
θ_{kref} (rad)	Fig. 7b	−0.052	−0.052
$\dot{\theta}_{\text{kref}}$ (rad/s)	time derivative of Fig. 7b	0.0	0.0

shortened or lengthened so that the walking cycle could be adjusted to a wearer's intentions or a wearer's body constitution.

On the other hand, a swing leg in the landing phase is supported by constant-value control for the preparation of patient's weight support. The reference angle and angular velocity in the landing and support phases are empirically set. Table 1 shows reference values in each phase of walking support. In this table, θ_{href} and $\dot{\theta}_{\text{href}}$ show the reference angle and angular velocity of a hip joint, respectively, and θ_{kref} and $\dot{\theta}_{\text{kref}}$ show the reference angle and angular velocity of a knee joint, respectively. In addition, the hip and knee joints should be straightened through the landing and support phase in order to support the wearer's weight by one leg. Therefore, the reference angle of hip joint in the landing phase is 0 rad. Table 1, however, shows the reference angle of the knee joint is not 0 rad but −0.052 rad. This over-extension of the knee joint can prevent the knee joint from bending due to the impact of landing a foot and gravity. In general, it is quite harmful for a human to extend the knee joint excessively, but HAL does not extend wearer's joints beyond the range of motion since the fastening equipment of HAL made of rigid plastic has the little flexibility and mechanical limiters at the knee joints prevent the joints from extending more than that angle. HAL controls the joint angle to keep the reference values in the support phase until the end of the single leg support phase when the foot of the opposite side swing leg touches on a floor. After the foot of the swing leg makes contact with the floor, the reference hip joint angle of the supporting leg switches from 0.0 to −0.7 rad shown in parentheses in Table 1. This hip extension contributes to the smooth weight shift from the current supporting leg to the following one. The reference angular velocity of both joints in the landing and support phase is consistently 0.0 rad/s through one cycle of walking support.

4.2. Intention estimator

Estimation of a patient's intentions contributes to providing not only comfortable support, but also safe support, because an inconformity between the robot suit motion and the patient motion results in his stumbling or falling. Instead of bioelectrical signals used for the control of the conventional HAL, the FRF is used for intention estimation of participant A who can control his weight balance using two canes with his hands. The FRF reflects the position of the COG and the COG

could be reliable information for intention estimation. For example, a leg could leave the floor and work as a swing leg safely if it does not support his/her weight.

HAL estimates which leg supports the wearer's weight when the wearer begins to swing the right or left leg and when he/she wants to stop walking. At first, for example, the right leg is considered to be the support leg when the foot contact condition:

$$f_{rh} > \alpha_{rh} \quad \text{or} \tag{1}$$

$$f_{rt} > \alpha_{rt}, \tag{2}$$

is satisfied, where f_{rh} and f_{rt} are the FRFs of the right foot heel side and toe side, respectively. In addition, α_{rh} and α_{rt} are thresholds to detect a landing of the right foot. In general, condition (1) is applied in advance of (2) since a healthy person puts the heel of the swing leg on the floor in advance of the toe. Patients with leg paralysis, such as participant A, however, have a foot weighed down and may put the toe of the swing leg on the floor in advance of the heel. Condition (2) is effective in detecting the landing in cases of paraplegia patients. On the other hand, the left leg is considered to be the support leg when the foot contact condition:

$$f_{lh} > \alpha_{lh} \quad \text{or} \tag{3}$$

$$f_{lt} > \alpha_{lt}, \tag{4}$$

is satisfied, where f_{lh} and f_{lt} are the FRFs of the left foot heel side and toe side, respectively. In addition, α_{lh} and α_{lt} are thresholds to detect landing of the left foot.

Second, for example, HAL estimates the intention that a wearer wants to swing the right leg when swing start conditions:

$$f_{rh} < \beta_{rh} \quad \text{and} \tag{5}$$

$$f_{rt} < \beta_{rt}, \tag{6}$$

are satisfied, where β_{rh} and β_{rt} are thresholds to detect the moment when each part of the right foot leaves the floor. On the other hand, HAL estimates the intention that a wearer wants to swing the left leg when swing start conditions:

$$f_{lh} < \beta_{lh} \quad \text{and} \tag{7}$$

$$f_{lt} < \beta_{lt}, \tag{8}$$

are satisfied, where β_{lh} and β_{lt} are thresholds to detect the moment when each part of the left foot leaves the floor. In this study, the following two constraint conditions are added to the above conditions for more stable estimation of the wearer's intentions:

(i) Do not start to swing a leg unless the foot of the opposite side leg is on the floor.

(ii) Do not swing the same leg sequentially.

HAL estimates the intention that a wearer wants to stop in his/her tracks if a certain time has passed before the swing start conditions (5) and (6) or (7) and (8)